MINERALOGICAL MAGAZINE, DECEMBER 1976, VOL. 40, PP. 827–41

A metallographic study of the disruption of the Cañon Diablo projectile

H. J. AXON AND W. R. D. COUPER
Metallurgy Department, University of Manchester, Manchester, M13 9PL

SUMMARY. A metallographic investigation of macro- and micro-structures, supported by microprobe examination, has been made on similarly sized (< *ca.* 200 g) individual Cañon Diablo meteorites of rim or plains type. Plains type specimens show heat alteration zones of the ablation type. They are extensively cracked in a brittle manner and in some instances the cracks are penetrated by ablation melt product. In all cases the cracks are now penetrated by terrestrial corrosion. Cohenite and schreibersite are cracked in a brittle manner. By contrast the rim type specimens are remarkably free of internal cracking or corrosion penetration. Instead the cohenite, schreibersite, taenite, and kamacite are transected by slip faults or shear displacements along the line of which all phases appear to have slipped in a non-brittle manner. These specimens have all been subject to shock loading and particular attention is paid to the effects of shock on sphalerite, on cloudy taenite, and on martensitic plessite.

Plains specimens have broken from the original projectile in a brittle manner well above the earth's surface. Rim specimens have been scabbed from the rear of the projectile as it penetrated the earth's surface. Some of the rim specimens show signs of being heated by the blast of the crater-forming explosion.

FRESHLY fallen iron meteorites usually have a heat alteration zone (h.a.z.) about 0·5–1·0 cm thick at the outer surface. This is produced during ablative flight through the atmosphere and is superimposed on the original pre-terrestrial structure. In most cases the final impact with the solid surface of the earth does not produce significant structural alteration in the meteorite.

By contrast the Cañon Diablo irons are the debris from a huge projectile, part of which hit the earth with sufficient energy to excavate an explosion crater about 1 km dia. The crater is of considerable age and all the Cañon Diablo irons have experienced terrestrial corrosion to some extent. A proportion of them have also been exposed to the massive energy release of the crater-forming event, although the majority of the specimens that are scattered on the plains around the crater seem to have escaped this type of damage.

It has become customary, when dealing with the metallic specimens of the Cañon Diablo meteorite, to distinguish between those specimens that are more or less randomly distributed, up to a radius of about four miles, on the *plains* surrounding the crater and those that are concentrated on the actual *rim* of the crater.

Plains specimens may vary in weight up to 500 kg and, according to Heymann *et al.* (1966) they tend to show only a 'lightly' shocked condition and from mass spectrometer measurements of cosmogenic rare gases they appear to have resided at a mean depth of 70–80 cm within the pre-terrestrial projectile.

Rim specimens, by contrast, tend to be smaller, with a mean weight of about 1 kg, they are 'moderately' or 'heavily' shocked and appear to have resided at a mean depth of about 130 cm inside the projectile.

In this context Heymann *et al.* (1966) define 'heavily' shocked meteorites as those showing completely recrystallized kamacite throughout the entire sample, with carbon diffusion zones around cohenite in at least part of the sample. These criteria imply shock pressures of at least 750 kbar in the entire sample. 'Moderately' shocked specimens are those in the pressure range 130–750 kbar. Heymann *et al.* (1966) used this class when un-recrystallized kamacite was present in any part of the sample (implying < 750 kbar at that location) and they drew attention to the existence of considerable gradients of shock effect within some specimens, as indicated by the presence or absence of such shock indicators as Neumann bands, acicular kamacite, recrystallized kamacite, carbon diffusion zones about cohenite, eutectic melting, or shock transformation of troilite. Lipschutz (1967) in his study of cohenite confirmed this observation of temperature or pressure gradients and also devised a scale of shock pressures based on the change of X-ray diffraction patterns in artificially shock-loaded cohenite, which at progressively increasing shock pressures show recrystallization without decomposition. This recrystallization effect in cohenite is especially valuable for the identification of shock events since it is not obtained by simple heating at constant low pressure. By contrast, the recrystallization of kamacite, carbon diffusion, or eutectic melting might be produced either by a shock wave or by heat alone at low pressure. In the complex situation of crater formation the possibility of a shock event followed by a separate reheating event must not be overlooked.

It is noteworthy that shock-induced diamonds are a feature of some rim specimens and also that moderately shocked specimens of the rim type have been encountered at distances of several km from the crater. These latter appear to belong to rays of throwout material and it is therefore convenient to distinguish between 'plains type' and 'rim type' samples according to their shock condition, irrespective of whether they actually reside on the rim or on rays of throwout material.

'Lightly' shocked material constitutes the overwhelming majority of plains specimens. It is characterized by the presence of Neumann bands, indicating a shock history less than 120 kbar. Moreover the Neumann bands are of earlier origin than the heat alteration zone which is present on all plains specimens (see Table I). Thus the Neumann bands in plains specimens are of pre-terrestrial origin and these specimens have somehow acquired an ablation type of heat alteration zone and have also escaped the shock of crater-forming impact.

In their comparative study of rim and plains material Moore *et al.* (1967) found that the interiors of rim specimens were effectively free of terrestrial corrosion product. By contrast they encountered about 3 % in plains specimens but they did not report on the detailed distribution of corrosion product in the structure.

Methods

The objectives of the present work were to investigate the modes of disruption of the Cañon Diablo projectile and to give a more complete account of some of the struc-

tural changes induced in the various phases of the meteorite by the thermal and mechanical processes that operated during the crater-forming explosion.

To this end small complete individuals of plains type and rim type iron were sectioned, metallographically examined, and compared. In order to make a valid comparison care was taken to select individuals of a similar size, and in the present work each complete individual weighed less than about 200 g. As the investigation progressed it appeared that the examination of a larger sample of rim material might prove instructive and in consequence the 250 g endpiece (34.6080) from a specimen of approximately 2 kg weight was examined and is reported on in a separate section.

The samples were obtained from the American Meteorite Laboratory and their catalogue numbers, individual weights, areas of examined section, and a brief indication of the important structural features are collected in Tables I and II. Sections were mapped in detail using the method of Axon and Waine (1972) and conventional metallographic examination of the Nital-etched sections was supported by polarized-light examination of shock structures in troilite, schreibersite, and cohenite. An A.E.I. microprobe was used for the identification of phases and on one plains specimen sulphur-printing was used to confirm the deep penetration of troilite melt-product within the macroscopic crack pattern.

The X-ray diffraction pattern of cohenite (also of kamacite or schreibersite) was obtained by carefully positioning the entire meteorite section in a specially constructed back-reflection camera so that the collimated beam of about 0·4 mm dia. was accurately positioned on the desired phase. This achieves the effect obtained by Lipschutz (1967) who chipped out fragments of cohenite and examined their high-angle reflections in a non-rotated Debye–Scherrer camera. Comparison of our back-reflection patterns with those obtained by Lipschutz from calibrated samples enabled an estimate to be made of the shock pressure in the cohenite and these values are recorded in Table II.

Results and discussion

Plains-type specimens

Observations on plains-type specimens are collected in Table I. Cañon Diablo samples show variable proportions of cohenite. In Table I the symbols C.R. and C.F. are used for sections of uniform structure that are cohenite-rich and cohenite-free respectively. When the section is not of uniform structure an attempt is made to represent the relative proportions of C.R. and C.F. areas. In general cohenite exists as elongated islands strung out along the centres of kamacite plates but it may also exist as a *swathing* layer about massive schreibersite. The symbols G and H represent, respectively, the breakdown of cracked cohenite to produce graphite and the presence of the cubic carbide $(Fe,Ni)_{23}C_6$, haxonite.

All of the plains-type individuals in Table I show a complete rim of corrosion product around the edge of the section. However, in none of the plains type specimens is the extent of surface corrosion sufficient to completely remove the h.a.z., relics of which may remain in quantities varying from trace (say 5 % of perimeter) to extensive (say 30 %). The presence of h.a.z. on plains-type specimens indicates that we are

dealing with complete individuals that experienced a period of independent high-velocity flight through the atmosphere.

A distinguishing feature of the macrostructure of the plains-type individuals is the very extensive penetration of terrestrial corrosion product parallel to the plates of the Widmanstätten structure. In several of the approximately 200 g specimens this corrosion extended right to the centre of the meteorite, so that when a thin slice was cut

TABLE I. *Plains-type specimens (all specimens have a layer of corrosion product on their outer surfaces).*

No.	Wt. g.	Area sq. cm.	Carbides	Sphalerite	h.a.z.	Internal corrosion	Melt product
Specimens with negligible mechanical distortion							
34.5125	168	11·8	C.R.	2	Trace	V. extensive	—
H37.246	61	2·7	C.R.	—	Trace	Extensive	—
H37.244	107	3·4	C.R. (G) trace H (unaltered)	1	Extensive	Moderate	Trace
34.5283	236	13·8	1/3 C.R. (G) 2/3 C.F.		Moderate	Moderate	Plentiful
34·5337	196	10·6	1/10 C.R. (G) 9/10	3	Moderate	V. extensive	—
34.6055	194	8	C.F. trace swathing C at edge	—	Moderate	Extensive	Trace
34.4695	331	11·3	C.F. trace swathing C at edge	2	Trace	Moderate	Trace
34·5141	125	3·8	C.F.	—	Extensive	Extensive	Plentiful
34.5219	35	2·1	C.F.	1	Trace	V. extensive	Trace
34.5216	150	6	C.F.	1	Trace	Extensive	Trace
Specimen showing considerable deformation, bending and twisting of structure and broad deformation bands in metal (no shear displacements)							
34.5279	85	4·1	C.F.	—	Extensive	Extensive I.C. also extensive at edge, and along deformation bands.	—

from it the kamacite plates fell apart like uncemented tiles in a mosaic. Microscopic examination showed that this '*internal corrosion*' of Table I was concentrated in the cracked filaments of schreibersite that are commonly present at the kamacite plate boundaries. An important observation of the present work is that the corroded remains of ablation melt product (melt product in Table I) are encountered deep within the crack pattern of at least seven specimens of plains-type individuals in Table I. This indicates that (at least some of) the macroscopic cracks were present before the individuals experienced their period of independent ablative flight and is consistent with Nininger's (1956) suggestion that the plains-type individuals of Cañon Diablo cracked away from the main mass of the projectile. The absence of severe shock structures and the presence of h.a.z. in these specimens suggests that the fragmentation took place by brittle failure, without compressive shock effects, when the projectile was passing through the earth's atmosphere. The cracked-off fragments would be retarded relative to the main mass of the projectile and their distribution about the

crater suggests that the trajectory of the main mass was essentially perpendicular to the earth's surface.

This stage of the Cañon Diablo fragmentation process is essentially the same as that deduced by Krinov (1966, 1974) for the Sikhote Alin event. In both instances the

TABLE II. *Rim type specimens (all specimens have a layer of corrosion on their outer surfaces but no 'internal corrosion').*

Meteorite number	Wt. g.	Area sq. cm.	Carbides	Condition of carbides			Sph.
				Optically visible recrystallization	X-ray shock pressure	Diffusion border	
34.5335	59	13·0	C.R. Swathing. H.	No	600 kbar	No	U. M.
34.5420	105	8·3	C.R. H.	On shear bands	600	Tenuous	U. M.
34.2677	138	4·7	¼ C.R. ¾ C.F.	On shear bands	700	Tenuous	M.
H37.62	69	6·0	Swathing round massive schreibersite and troilite (G)	Partial	< 800	Tenuous	M.
34.5422	41	1·9	C.R. (G)	On shear bands	800?	Distinct (21)	—
34.5421	61	2·1	C.R. Swathing	General	1000	Distinct (11)	—
34.FRI	24	1·8	C.R.	General	> 1000	Distinct (13)	M.
34.2731	217	14·9	½ C.R. ½ C.F.	General + shear bands	> 1000	Distinct (27)	—
34.2737	214	4·7	½ C.R. ½ C.F.	General	1300	Distinct (16)	—

Meteorite number	Schr.	Visible shear displacements	Condition of kamacite	Condition of taenite or plessite
34.5335	U	α γ C	N. ε patches. Rextln. only at shear zones and ZnS	Shock altered martensit Cloudy γ
34.5420	U	α γ C	Rextl. N. Rextl. ε. Rextln at shear zones.	Shock altered martensite Cloudy γ almost removed
34.2677	1–2	α C	Rextln. N. Rextl. of ε almost complete.	Shock altered martensite Clear γ Cloudy γ almost removed
H37.62	2	no	Recrystallized α variable grain size few phantom Ns.	γ almost cleared
34.5422	2–5	γ	Recrystallized	Clear white γ
34.5421	2–5	(γ)	Recrystallized	Clear white γ
34.FRI	2	γ C	Recrystallized	Clear white γ
34.2731	3–6	γ C	Recrystallized	Clear white γ
34.2737	2	γ C	Recrystallized	Clear white γ

No. 34.5335 shows no thermal gradients; nos. 34.5422, 34.5421, and 34.2731 do.

fragmentation is predominantly brittle as a consequence of the distribution of brittle schreibersite along the edges of the plates (or grains) of kamacite. However, by comparison with Cañon Diablo the Sikhote Alin structure is much coarser, its trajectory more inclined, it underwent several identifiable stages of fragmentation, and its total mass was insufficient to produce an explosion crater on the Arizona scale.

In addition to the filaments of schreibersite at the edges of the kamacite plates the Cañon Diablo material also contains brittle phases that are less likely to produce

continuous and extensive cracking paths through the bulk of the meteorite. In particular there are small idiomorphic rhabdites embedded within the kamacite and occasional large, but discontinuously distributed non-idiomorphic (massive) schreibersite. Cohenite particles are also present in some specimens but these are located at the centres of kamacite plates, not at their boundaries, and so do not directly contribute to the development of the macroscopic (grain-boundary) cracking pattern. Microscopic examination of the cohenite and of any massive schreibersite that is present in plains-type specimens shows that both of these phases are invariably cracked. In the first ten instances of Table I these massive compound phases have cracked in a brittle, cataclastic, manner to form an 'internal breccia' that consists of relatively large blocks of slightly displaced fragments but with no over-all change in the external shape of the brittle phase. The brittle nature of the cracking is confirmed by the sharp X-ray diffraction spots obtained from the individual blocks of cohenite and schreibersite and by the uniform extinction of the cohenite in polarized light, indicating the absence of strain within the fragmented blocks of cracked compound. In these specimens there is usually no over-all bending, twisting, or macroscopic deformation of the metal phases. Indeed the individual kamacite plates have separated without macroscopically visible deformation and the Neumann bands within the kamacite are straight and undeformed. It is therefore permissible to say that not only have the individual particles of compound phases cracked in a brittle manner but also that this totally brittle cracking behaviour has extended to the complex metal-compound aggregate that constitutes the whole structure in these ten small plains specimens.

Attention should now be paid to the last specimen in Table I. This is a plains-type specimen as is shown by the extensive h.a.z. and internal (grain boundary) corrosion. However, the kamacite and taenite in this specimen show considerable mechanical distortion, which varies in magnitude from a mild bending of Neumann bands to broad zones of deformation in the kamacite and bending and folding of the taenite. There are no sharp physical displacements of structure (i.e. *no* slip faults) since the deformation takes the form of over-all bending rather than local shearing and the zones of deformation are quite wide. Corrosion seems to have attacked areas where the deformation has been intense and has invaded several large zones of kamacite deformation. However, at least one such zone of deformation remains uncorroded and is intersected by the h.a.z.—indicating that the deformation was of earlier origin than the h.a.z. The schreibersite in this specimen is finely comminuted with pronounced relative displacement of the fragments and there is often an over-all change in the outline of, or large-scale folding of, the crushed schreibersite, thus allowing it to accommodate itself to the plastic flow of the surrounding metal.

The presence in this specimen (34.5279) of kamacite boundary cracking, internal corrosion penetration, and Neumann bands suggest that the plastic deformation and folding were superimposed on an earlier brittle cracking pattern. Thus it is possible that this specimen was originally similar to the other ten in Table I but was subsequently torn into secondary fragments by tensile or bending processes, which, however, also operated while the material was still in ablative flight.

Reheating features. Reference to Table I indicates that in three instances the cohenite

has commenced to decompose to graphite and metal at crack locations. An identical effect was reported by Heymann *et al.* (1966) who ascribed it to a mild secondary reheating probably when the sample fell on to hot ejecta from the crater. No evidence of reheating was encountered in the bulk kamacite or schreibersite in agreement with the observation of Brentnall and Axon (1962) that graphitization at cracks is a sensitive indicator of reheating. A small quantity of haxonite (H) was encountered in sample H37.244 without any metallographically visible signs of reheating. Likewise no reheating effects were detected in the cloudy taenite of any plains-type individuals other than within the h.a.z. where severe local heating tended to remove the cloudy feature to produce the reticulated or clear taenite of Brentnall and Axon (1962).

Small idiomorphic and thermally unaltered crystals of sphalerite were encountered occasionally and their sightings are recorded in Table I.

Thus to summarize, the fragmentation and crack patterns of Cañon Diablo plains specimens are controlled by the distribution of brittle schreibersite along the edges of the kamacite plates. The h.a.z. indicates a period of ablative flight for the individual meteorite fragments and the penetration of ablation melt product indicates that the brittle cracks were present during that flight. Heymann *et al.* (1966) have produced evidence from cosmogenic rare-gas contents to indicate that plains specimens were originally part of the main projectile before it encountered the earth's atmosphere. It would therefore seem that plains-type specimens were stripped off from the outer layers of the projectile as it penetrated the atmosphere. At this stage of fragmentation there was no significant shock compression and the whole structure responded in a brittle manner when it encountered the atmosphere. The Neumann bands certainly predate the h.a.z. but on present evidence it is not possible to say whether they were already present in the main mass before it encountered the atmosphere or whether they were produced as a result of atmospheric disruption. Thus we still do not have unambiguous evidence concerning the presence or absence of metallographic effects arising from the earliest stage of disruption, i.e. when the main mass of the projectile was excavated from its parent body. All that we can say is that this major event was not accompanied by major shock damage to the metal. In turn this suggests that the metal was originally a 'raisin' embedded in silicate and the silicate absorbed the damage of primary excavation from the parent body.

After separation from the main projectile the plains specimens were decelerated by atmospheric friction and therefore arrived at the earth's surface later than the main projectile. The unburied irons were presumably the latest to reach the earth and most of them are free of deep-seated heating effects. However, the incipient graphitization of three of the specimens suggests that these may have landed upon and been slightly heated by hot ejecta from the crater. From the observations of Brentnall and Axon (1962) a temperature of less than 400 °C seems to be indicated.

Rim type specimens

Nininger (1956) has indicated that a distinguishing feature of rim-type individuals is a general diffuseness of the etched macrostructure as a consequence of reheating and Heymann *et al.* (1966) and Lipschutz (1967) have drawn attention to the frosty

patches that may appear in the macrostructure as a result of shock gradients. However, no previous detailed consideration appears to have been given to the pattern of cracking or corrosion effects in rim-type material.

The small individual rim-type specimens examined in the present work are listed in Table II in increasing order of shock intensity as estimated from the X-ray diffraction pattern of the cohenite, using the pressure scale calibrated by Lipschutz (1967). It should be noted that all of the rim-type specimens of the present work contained at least some cohenite. Cohenite in rim-type specimens is *not* cracked.

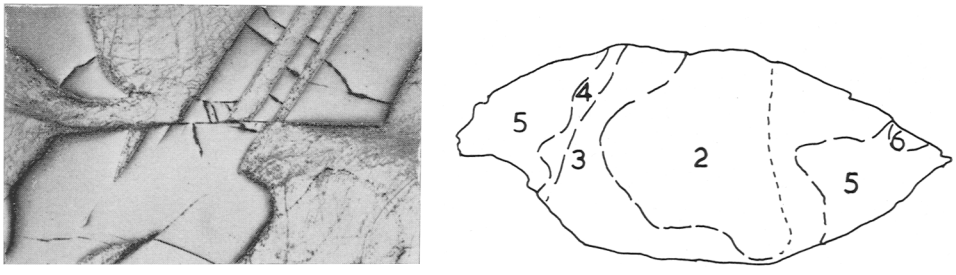

FIGS. 1 and 2: FIG. 1 (left). Shear displacement or slip fault in the cohenite of specimen 34.2677. Etched 2 % Nital. Field of view 1·4 mm × 1·0 mm. Note the sharply defined translation of the two portions of the massive cohenite and the flow structure that has etched up in the metal. FIG. 2 (right). Temperature contours on a section of sample 34.5422 as determined from the metallographic identification of heating effects on phosphide inclusions. Phosphide types 2–6 are defined in the text. Maximum length of section 2·4 cm.

All of the slices taken from rim-type specimens are entirely free from the macroscopic crack penetration that is such a universal feature of the plains-type specimens. Correspondingly they show no penetration of corrosion product (internal corrosion) into the depths of the Widmanstätten structure. They show an apparently similar degree of section-edge corrosion to that encountered in plains specimens but careful microscopic examination of the edges of rim-type specimens has in no case revealed h.a.z. of the ablation type. There is of course no penetration of ablation melt product. Observations on rim-type specimens are collected in Table II.

Shear displacements: slip faults. When the rim-type specimens were subjected to systematic microscopic examination and the microscopic features mapped, it became clear that in effectively all of the rim specimens there was evidence of very sharp shear displacements (slip faults) in the carbide, phosphide, taenite, or plessite particles (fig. 1). Furthermore, when these structural features were mapped the sharp shear displacements in the taenite and compound particles tended to line-up to mark lines of slip-faulting that sometimes extended continuously through the meteorite for several cm. In some of the least heavily shocked specimens it was possible to follow the line of the fault through the kamacite also. However, in the more heavily shocked specimens the general recrystallization of the kamacite (Table II) had obliterated the trace of the fault line in that phase. These shear displacements in Cañon Diablo have been figured by Perry (1944) and discussed by Axon (1969). Perry did not make it clear

whether the effect was restricted to rim-type specimens, but from the present work it is clearly so.

X-ray and microstructural studies. Rim specimens all show evidence of metamorphic phase changes and of heating effects that are consistent with an interlude of compressive shock. Some of the metallographic features are reported in Table II and, although shock intensities may not be homogeneously distributed throughout an individual specimen, there is over-all agreement between the metallographic features and the shock intensity as deduced from the X-ray diffraction pattern of the cohenite.

In kamacite the range of microstructures extends from Neumann bands (N in Table II), with or without recrystallization, embraces shock hardened kamacite (ϵ) that may or may not show signs of local or general reheating and extends to fully recrystallized kamacite (α). The ϵ is an unambiguous indication of shock. The recrystallized kamacite may have arisen from high-intensity shock or from the secondary reheating of less heavily shocked material.

Effect of temperature on compound phases. The rise of temperature that accompanies compressive shock loading manifests itself somewhat differently in schreibersite and in cohenite.

Under the influence of progressive heating schreibersite diffuses into the surrounding kamacite and eventually, as the eutectic temperature is reached, it forms a metal–phosphide melt. The alteration is progressive and depends on time as well as temperature. However, it is possible to recognize six reasonably distinct stages of alteration and these are recorded for each specimen in Table II. Schreibersite type 1 (or U) is in the uncracked and thermally unaltered condition. Type 2 corresponds to the solid-state diffusion of Ni and P into the kamacite to produce thorn-like projections. Stage 3, the first detectable signs of melting; 4, half melted; 5 eutectic without excess metal; 6, dendrites of excess metal in a eutectic background. Types 3–6 might arise either by treatment at progressively higher temperatures or by exposure to a high temperature for increasing periods of time. However, within any single fragment of meteorite the changes will be self-consistent and may be used to map thermal contours within the meteorite. An example is shown in fig. 2.

Both schreibersite and cohenite in rim-type specimens are remarkably free from cracks. Instead they may show strain or recrystallization effects when examined by X-rays or polarized light. Thus in rim specimens cohenite lacks the opportunity to decompose to graphite at crack locations. Instead carbon diffuses from the cohenite into the surrounding metal, thereby producing a series of carbon diffusion zones the width of which depends on time and temperature of heating. The diffusion border is tenuous at low shock levels but becomes more distinct at higher shocks. The nature and approximate width, in μm, of diffusion border around cohenite near the centre of the specimens is recorded in Table II. However, within any one fragment of meteorite the extent of diffusion may vary from one location to another and may be used to plot thermal contours in a similar manner to that already described for schreibersite. In general, in rim type specimens of Cañon Diablo the contours indicated by schreibersite type run parallel to those indicated by the amount of carbon diffusion from cohenite.

Lipschutz (1967) has drawn attention to the gradients of shock pressure effects

that may arise in rim-type specimens of Cañon Diablo but in addition to gradients of shock pressure within the fragments it must be remembered that the rim-type fragments were formed near ground level during the excavation of the explosion crater. They were therefore in danger of secondary reheating from the hot blast of the crater-forming event. In the present investigation a number of rim type specimens did show concentric zones of heat treatment consistent with secondary blast heating. In other cases the gradients are more ambiguous and could be shock gradients or fragments of blast-heated material that had disintegrated after the heating event.

Reheating of a large rim-type specimen. The possibility of rim-type fragments being exposed to secondary reheating in the hot gases of the crater-forming explosion is shown particularly well in the 250 g endpiece 34.6080 which was received from the American Meteorite Laboratory as a 'cut and polished end section' from an individual of total weight about 2 kg. The material is cohenite-rich with islands of cohenite conventionally located at the centres of kamacite plates and in addition swathing cohenite about a substantial lath of schreibersite. As in the smaller rim-type specimens there is no cataclastic cracking of schreibersite or cohenite and no penetration of corrosion along plessite or kamacite grain boundaries. The kamacite is completely recrystallized and consequently the sharp shear displacements of the plessite and compound phases are not linked by visible fault lines on the kamacite.

Heat alteration effects in the compound phases vary according to location within the specimen. At the centre of the section, fig. 3, the grain-boundary schreibersite is Type 2; there are narrow zones of carbon diffusion at cohenite-kamacite interfaces and no visible interaction can be detected at cohenite-phosphide interfaces. These heating effects increase progressively towards the outer part of the section, where Type 6 schreibersite is found; there are wide zones of carbon diffusion and complex phosphide–carbide eutectic melts have formed at cohenite-phosphide interfaces. In fig. 3 the contours are plotted according to schreibersite type and the widths of carbon diffusion zones about cohenite. The contours are concentric and are superimposed on a pre-existing shocked structure. They represent a considerably deeper penetration of heat than is encountered in a conventional h.a.z. There are no signs of ablative melting and the depth of heat penetration is consistent with exposure of the specimen for about three seconds to a surface temperature of $\approx$ 1200 °C. This is the sort of heat treatment that might be expected to accompany the flight of a shocked sample through the hot gases of the crater-forming explosion.

Shock effects in Cañon Diablo

In the experimentally ideal case when a single plane shock wave passes a point in a homogeneous medium the instantaneous pressure and temperature at that point increase sharply to peak values, after which the peak pressure relaxes. The temperature falls to a residual value that is higher than the pre-shock temperature by an amount representing the thermal energy introduced by the shock process.

However, in the disruption of a meteorite by earth impact the situation is more complicated. For instance, the event will involve non-planar geometry and a number of intersecting shock waves may be involved. Indeed, Shoemaker (1963) has argued

that the survival of fragments of unfused material derived from the rear of the projectile arises because they escape the maximum shock pressures owing to the interaction of the shock front with rarefaction waves reflected from the sides of the projectile. Under these circumstances the mechanical adjustments of the meteoritic projectile during disruption will involve macroscopic shearing or tearing components in addition to simple pressure effects. Moreover, the loading in addition to being intense is also extremely (explosively!) rapid. The rim specimens of Cañon Diablo have obviously been subject to these very complex and rapidly applied systems of disruptive force and as a consequence they contain internal shear displacements or slip faults that are absent from the plains-type specimens.

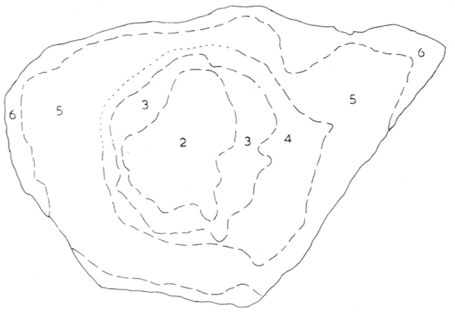

FIGS. 3 and 4: FIG. 3 (left). Temperature contours on the large rim-type specimen 34.6080. Legend as for fig. 2. Maximum diameter of this section 4·8 cm. FIG. 4 (right). Recrystallization along a shear displacement or slip fault in a schreibersite crystal of specimen 34.6080. Field of view 0·75 mm × 0·55 mm. Polarized light, reflected mode. The crystal of phosphide is dark and occupies most of the field. Metal to right or left of the phosphide shows light. The light band running through the phosphide is a band of recrystallization produced by shear displacement. The dark cracks are of later origin and cut through the band of recrystallized phosphide.

If the shocked medium is not single phase and homogeneous there will be intensification of local shock effects at interfaces where materials of different compressibilities meet. The Cañon Diablo meteorites are multiphase structures that are predominantly kamacite but contain up to 4 % taenite or plessite. The samples studied in the present work also contain cohenite, schreibersite, sphalerite, and occasionally troilite. Also it is well known that graphite and silicate phases, as well as cavities, have been encountered in other specimens.

The aim of the present section is to report briefly on a number of shock effects that are encountered in rim-type specimens of the Cañon Diablo iron, particularly in relation to the occurrence of shear displacements and the shock alteration of sphalerite, cloudy taenite, and martensitic plessite.

Shear displacements. In rim-type specimens there is no cataclastic fragmentation of cohenite or schreibersite and no bending, twisting, or macroscopic plastic deformation is visible in the metal phases. Instead they show shear displacements or slip faults. The line of the fault may run without discrimination both through the ductile metal phases (kamacite, taenite, plessite) and through those compound phases (schreibersite, cohenite) that are normally considered to be brittle. The fault line may extend for

several cm without deviation. Where the fault line crosses a particle of cohenite or schreibersite the compound is sharply displaced along the line of the fault by distances ranging from a few μm up to about one mm. There is a remarkable absence of cracking of the compound phases, both in the immediate vicinity of the shear displacement and generally. Indeed, polarized light examination of the compounds sometimes shows a recrystallized structure, which may be particularly well developed along the trace of the shear displacement (fig. 4). The details of the shear displacement in the kamacite are best seen in the two samples at the top of Table II. In those samples the bulk of the kamacite has a shock-hardened structure that has not been subject to over-all recrystallization. In the etched section the line of the fault in these specimens shows up in the kamacite as a 'mylonitized' layer of fine-grained recrystallization several μm thick. These specimens are particularly valuable for the information they give about the progress of the fault through the kamacite matrix, since, in addition to showing the trace of the sharply defined main shear displacement, the etched kamacite also shows how intersecting fault planes interact with one another and how the ends of sharply defined fault planes degenerate into diffuse fans of deformation flow, like a river delta. In this way the intense shear of the main fault plane is gradually accommodated to the unsheared bulk of the specimen without the need for catastrophic discontinuities in the material. Accommodation shears may also be detected along the length of some main fault planes. In the non-recrystallized bulk kamacite of these specimens the shear and accommodation effects appear to be superimposed on, and therefore formed later than, the shock-hardened bulk of the kamacite. They are therefore consistent with shearing movements arising from the presence of unbalanced forces in the projectile as it adjusts itself to the passage of the complex shock waves.

Where the fault line crosses a particle of taenite the two displaced halves of the taenite may be connected along the line of the fault by a thinly drawn-out continuous strand of taenite, while in heavily shocked samples partly melted sulphide or phosphide is sometimes strung out along the line of the fault. These metallographic effects indicate intense local heating of the fault plane while the shear displacement was in process of formation. Indeed, the presence of small-grain recrystallized kamacite or partly melted eutectics would act as a lubricant to keep the fault plane active once it had started to slip. The circumstances under which the displacements are *initiated* are less certain. A number of alternative mechanisms may be available. However, when a fault plane cuts cohenite or schreibersite it always appears to make a sharp planar cut. The 'mylonitization' zone often becomes thicker in the adjacent kamacite. These effects suggest that on at least some occasions the displacement is initiated in the compound and spreads from there into the metal. In any case it is clear that the rim-type fragments were broken away from the rear of the projectile by means of a shock event in the course of which the preferred mechanism of deformation in the compound phases was local shear by flow on a slip plane instead of the extensive brittle fracture that is more usually encountered under conditions of impact loading when shock compression is not present.

Sphalerite. As indicated in Table I, trace quantities of sphalerite were encountered in most of our small plains specimens. It was usually idiomorphic in the size range

20–200 μm and located at the centres of kamacite plates. It was also encountered within or at the edge of cohenite or in contact with schreibersite. Probe analyses of seven unaltered particles in plains specimens gave an iron plus zinc content that lay between the compositions FeS and ZnS and had Zn contents in the range 49·2–54·5 wt. %.

Similar quantities and distributions of sphalerite were encountered in the rim specimens. However, as may be seen from Table II, in the more heavily shocked specimens the originally idiomorphic crystals have been transformed into irregular patches of eutectic melt-product (M in Table II). In the less shocked specimens melting is incomplete, so that unaltered (U) sphalerite may exist in contact with melted material. In the least shocked specimen 34.5335 melting of sphalerite is accompanied by local recrystallization of the interface kamacite, thus indicating a higher effective shock temperature at the sphalerite than within the bulk of the metal. The slightly more heavily shocked specimen 34.5420 contains the complex association of unmelted sphalerite in cohenite with cohenite–kamacite–sphalerite melt product that is shown in fig. 5. In this specimen the melted area analyses at 17·1 wt. % Zn, 60·4 wt. % Fe, 17·1 wt. % S, 2·1 wt. % Ni, and also contains an unmeasured quantity of carbon. This composition is in agreement with the microstructure of fig. 5 which suggests that sphalerite melt-product has dissolved both cohenite and kamacite. In this and several other specimens sphalerite melt-product has penetrated along cohenite–kamacite phase boundaries. Also in specimen 34.5420 sphalerite was found reacting with schreibersite to give a melt product containing 11·7 wt. % Zn, 47·3 wt. % Fe, 14·8 wt. % S, 13·8 wt. % Ni and 12·4 wt. % P.

Cloudy taenite and martensitic plessite. Scott (1973) found the cloudy border that forms in taenite between 32 and 42 wt. % Ni to consist of an optically submicroscopic cellular structure, analogous to a foam in which the soap film corresponds to kamacite and the enclosed volumes are taenite. The cloudy structure forms by the decomposition of taenite, probably below about 400 °C, and the decomposition may be assisted by the presence of dissolved carbon. Reheating to about 800 °C, as in h.a.z., dissolves the cellular structure and removes the cloudy feature, which is replaced by 'white' taenite. Lesser degrees of reheating produce a patchy or reticulated appearance in the cloudy taenite. This range of structures is well known in h.a.z.'s but Scott (1973) has also commented on the patchy dissolution of cloudy taenite within the bulk of an impact-heated specimen of Cañon Diablo.

The rim-type samples in Table II all show some degree of alteration to cloudy taenite. It is entirely absent from the most heavily shocked samples and is replaced by structureless clear-white taenite. An example is shown in fig. 6, from which it may be seen that the clear-white taenite is surrounded by a zone of carbon enrichment in the kamacite showing that under the influence of sufficiently intense shock heating carbon may escape from the cloudy taenite and diffuse into the kamacite. With less intense shock the cloudy feature may be removed but with no diffusive loss of carbon from the taenite, which is then not completely white, but shows the faint straw-coloured needles that are characteristic of freshly formed carbon martensite.

However, when the shock has not been sufficient to produce recrystallization of the kamacite there may be an intensification and extension of the cloudy structure. An

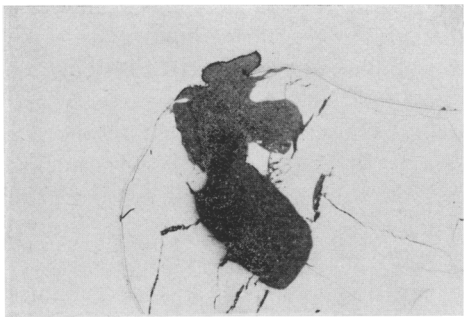

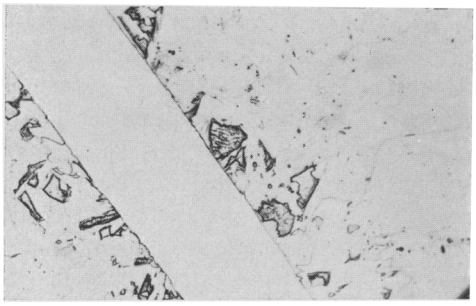

FIGS. 5 and 6: FIG. 5 (left). Cohenite, light, cracked with a tenuous carbon diffusion border to kamacite, specimen 34.5420. Within the cohenite unmelted sphalerite is present as a dark area. Melted sphalerite is present as a mottled area of amoeba shape at and below the cohenite–kamacite interface. Field of view 1·0 mm × 0·7 mm. FIG. 6 (right). Structureless, clear white taenite. Originally cloudy taenite, which has been cleared by shock heating. Note the diffusion of carbon into the surrounding kamacite. Specimen 34.6080. Field of view 0·2 mm × 0·14 mm. Etched 2 % Nital.

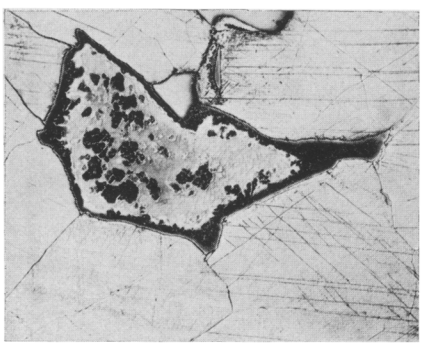

FIGS. 7 and 8: FIG. 7 (left). Shock altered martensitic plessite in sample 34.5335. Etched 2 % Nital. Field of view 1·0 mm × 0·75 mm. Shock has intensified the dark etching borders to the plessite field and has transformed some of the interior plessite (originally martensite with about 13 % Ni) into dark etching, cloudy, taenite. FIG. 8 (right). Shock altered martensitic plessite in sample 34.2677. Etched 2 % Nital. Field of view 1·0 mm × 0·7 mm. Shock pressures intermediate between those of figs. 6 and 7 have produced a patchy structure. Cloudy taenite is removed but carbon has not diffused from the taenite into the surrounding kamacite.

example from specimen 34.5335 is shown in fig. 7. The relatively low shock intensity in this specimen is accompanied by only slight heating in the bulk of the metal. In specimen 34.5335 the cloudy borders of taenite are unusually wide and etch more darkly than in unshocked plains specimens. Microprobe examination of these extended dark borders show that they are present down to about 13 wt. % Ni in contrast to the lower limit of $\approx$ 30 % for cloudy taenite in unshocked material. In addition (fig. 7) round patches of cloudy structure have developed, away from the dark border, within the mass of the original plessite field. Successive repolishing and re-etching shows that these rounded patches are globules—not plates—and microprobe examination shows them to contain about 13 wt. % Ni, with no detectable change of nickel

content between the dark patches and the martensitic matrix within which they occur. Thus it appears that in rim-type specimens such as 34.5335 the shock event generated a combination of circumstances conducive to the extension rather than the removal of the cloudy feature.

From the work of Rhode (1970) on homogeneous martensitic alloys of iron, nickel, and carbon it is known that shock can cause martensite to transform to austenite (taenite). For a homogeneous alloy containing 30 wt. % Ni, 0·1 wt. % C at 45 °C a transformation pressure of 67 kbar has been reported. Higher pressures would be required for a 13 wt. % martensite and the shock response of multiphase $\alpha+\gamma+$ compound material has not been investigated. However, it is clear that the microstructures of fig. 7 are consistent with a cycle of events in which the normal martensitic plessite of unshocked Cañon Diablo was transformed by shock to taenite. On cooling from the shock, part of this shock-induced taenite decomposed to cloudy taenite, but at lower temperatures the alternative transformation to martensite occurred. It appears that under these favourable conditions the cloudy feature may develop rapidly, since in the shocked fragment it appears to have formed while cooling from the residual temperature of about 350–400 °C (Heymann *et al.*, 1966). In unshocked meteorites, under the usual conditions of slow cooling, the cloudy taenite border appears to form below about 400 °C also. However, nothing is known about the speed at which it develops in unshocked material. Kimball (1973) has suggested that even in the unshocked material the cloudy feature is instigated by a small internal stress.

More intense shock levels, sufficient to produce recrystallization of the kamacite matrix but not sufficient to produce completely white taenite, may also give rise to a patchy structure in shocked fields of martensitic plessite but in these cases, specimen 34.2677 of Table II, fig. 8, cloudy taenite does not survive the shock event. These effects are recorded in Table II as Shock altered martensite.

REFERENCES

AXON (H. J.), 1969. In *Meteorite Research*, ed. MILLMAN (P. M.), pp. 796–805. Dordrecht (D. Reidel).
—— and WAINE (C. V.), 1972. *Min. Mag.* **38**, 725.
BRENTNALL (W. D.) and AXON (H. J.), 1962. *Journ. Iron Steel Inst.* **200**, 947.
HEYMANN (D.), LIPSCHUTZ (M. E.), NIELSON (B.), and ANDERS (E.), 1966. *Journ. Geophys. Res.* **71**, 619.
KIMBALL (M. R.), 1973. *Meteoritics*, **8**, 397.
KRINOV (E. L.) [Кринов (Е. Л.)], 1966. *Giant Meteorites* (Pergamon).
—— 1974. *Meteoritics*, **9**, 255.
LIPSCHUTZ (M. E.), 1967. *Geochimica Acta*, **31**, 621.
MOORE (C. B.), BIRRELL (P. J.), and LEWIS (C. F.), 1967. Ibid. **31**, 1885.
NININGER (H. H.), 1956. *Arizona's Meteorite Crater*. Amer. Meteorite Mus., Sedona, Arizona.
PERRY (S. H.), 1944. The Metallography of Meteoric Iron. *U.S. Nat. Mus. Bull.* **184**, Plate 75.
RHODE (R. W.), 1970. *Acta Met.* **18**, 903.
SCOTT (E. R. D.), 1973. *Geochimica Acta*, **37**, 2283.
SHOEMAKER (E. M.) 1963. In *The Moon, Meteorites and Comets* ed. MIDDLEHURST (B. M.) and KUIPER (G. P.) (Vol. IV of the Solar System), 301–36. University of Chicago Press.

[*Received 22 December 1975*]